Supporting Information

Montgomery *et al.* 10.1073/pnas.0810241105

SI Text

Transgene Construct Design and Development. Syn-tasiRNA sequences were designed to contain a 5′U and to target distinct regions of *PDS* mRNA. *TAS1c*-based syn-tasiRNA sequences were substituted for tasiR255 and tasiR850 at positions 3′ D3(+) and 3′D4(+) of *TAS1c*, respectively. The syn-tasiRNA in the 3′D3(+) position was the same for each of the *35S*:*TAS1cPDS-1*, *35S*:*TAS1cPDS-2*, and *35S*:*TAS1cPDS-3* constructs, but the syn-tasiRNA in the 3′D4(+) position was different (Fig. 1*A*). The *35S*:*TAS1cPDS-4* construct contained two unique syn-tasiRNA sequences, both with 3′ ends designed to result in three target site mispairs to suppress transitive silencing effects (Fig. S1*A*) (1).

The *TAS1c* transcribed region was amplified from genomic DNA by using the following primers: TAS1c_F [caccAAACCTAAACCTAAACGGCTAAGC] and TAS1c_R [ATTTCACTTTACGATGTGGTG]. Syn-tasiRNA sequences, miRNA target site mutations, and internal and 5′ and 3′ deletions were introduced into *35S*:*TAS1cPDS-2* by site-directed PCR mutagenesis (2). *GFP* sequence was amplified from *pRTL2 smGFP* plasmid DNA (3). miRNA target sites and *TAS1c* sequence were introduced into the *GFP* sequence via PCR. *MIR171a* and *MIR173* were amplified from genomic DNA by using the following primers: MIR171a_F [caccTGCTCCATACCTTCCATTTCC] and MIR171a_R [GGCAAGGAAGCTGATTAAGGG]; MIR173_F [caccATAATTAGCAAGTAATAAGG] and MIR173_R [ATCTGTTATACAACCAAATCC]. The "cacc" sequence at the 5′ end of each forward primer was for cloning purposes. PCR products were cloned into pENTR/D-TOPO (Invitrogen), followed by recombination into pMDC32, a plant transformation vector containing a 35S promoter and nos terminator (4). To generate the dual-gene construct *35S*:*TAS1cPDS*/*173*, a nos terminator and 35S promoter were introduced upstream of *MIR173* by site-directed PCR mutagenesis. The resulting PCR product was cloned into pENTR/D-TOPO. The *TAS1cPDS-4* sequence was then ligated upstream of the *nos-term-35S*:*MIR173* cassette and recombined into pMDC32, such that the 35S promoter of the pMDC32 vector drove expression of *TAS1cPDS-4* and the nos terminator of pMDC32 provided the termination signal for *35S*:*MIR173*. Pfu Ultra or Pfu Ultra II polymerase (Stratagene) was used for all PCRs.

Plants and Growth Conditions. *rdr6–15*, *dcl4–2*, *zip-1*, *dcl1–7*, *hyl1–2*, *se-2*, *hen1–1*, *hst-15*, *ago1–25*, *ago1–36*, *ago2–1*, *ago3–1*, *ago4–1*, *ago5–2*, *ago6–1*, *ago6–2*, *zip-1*, and *ago8–1* alleles have been described (5–18). The *ago9* (SALK_126176, insertion in intron 11) and *ago10* (SALK_019738, insertion in intron 15) alleles were obtained from The Arabidopsis Biological Resource Center (19). Homozygous mutant plants were generated and confirmed by PCR-based genotype analysis. Plants were transformed by floral dip by using *Agrobacterium tumefaciens* GV3101 (20) and selected on MS medium containing hygromycin (50 μg/ml). Plants were transferred to a greenhouse with a 16-h light/8-h dark supplemental light cycle.

Transient Expression. Transient expression in *N. benthamiana* leaves was done as described (21) with *Agrobacterium tumefaciens* GV3101. When multiple constructs were coexpressed, equal amounts of each *Agrobacterium* strain were used within each experiment. The final concentration of *Agrobacterium* before injection was adjusted to an OD_{600} of 1.0 by using cultures containing empty vector. RNA was isolated 48 h postinfiltration.

RNA Assays. RNA was isolated by using TRIzol reagent (Invitrogen). Three chloroform extractions were done and RNA was precipitated in 0.5× isopropanol for 20 min. Duplicate or triplicate samples from pools of independent primary transformants or infiltrated leaves of *N. benthamiana* plants were analyzed. For high-molecular weight (HMW) RNA blot assays, 5 μg total RNA was resolved by denaturing 1.5% agarose-gel electrophoresis. For small RNA blot assays, 10 μg total RNA was resolved by denaturing 17% PAGE. In most cases, RNA standards were run in parallel. RNA was transferred to positively-charged nitrocellulose membranes. DNA probes were randomly labeled by using ^{32}P-dATP and Klenow fragment. DNA and LNA oligonucleotide probes were end-labeled by using [^{32}]ATP and Optikinase (USB). Probes were hybridized to RNA on membranes in Sigma Perfect-Hyb Buffer at 68° (HMW blots) or 38° (small RNA blots). An Instant Imager (Packard Bioscience) was used to measure blot hybridization signals.

Quantitative RT-PCR using the following *PDS* and *ACT2* primers: PDS_F [GAACAACGAGATGCTGACATG] and PDS_R [TTCCAGGGATCTGGTAAAAGGAG]; ACT2_F [GCCATCCAAGCTGTTCTCTC] and ACT2 R [GAACCACCGATCCAGACACT], were done as described (22). Modified RNA ligase-mediated 5′ RACE assays were done as described (21) using the following gene-specific primers: TAS1c_5′_RACE [AGCAACTGTTCTTTAGACGACTTGAAAATCTCAT]; TAS1cPDS-2_5′_RACE [CTAGTTCTGGCTGCGTCTGGACC] or TAS1c_707_5′_RACE [GATGATGCTTCTTCGCTACACCTCGGAGA]; GFP_5′_RACE [GGGCAGATTGTGTGGACAGGTAATGG]. 3′ RACE for mapping the 3′ ends of *35S*:*TAS1cPDS-2* and endogenous *TAS1c* transcripts was done as described (23) with the following gene-specific PCR primers: TAS1c_3′_RACE [CTAAGTTCAACATATCGACGAACTAGA] and TAS1cPDS-2_3′_RACE [CTTGGTCCAGACGCAGCCAGAAC].

Small RNA Sequencing. Small RNA amplicons were prepared as described (22). Sequencing-by-synthesis (SBS) was done with an Illumina 1G Genome Analyzer. Twenty-one-nucleotide small RNA reads from *Arabidopsis* endogenous *TAS1c* or *N. benthamiana* expressing *35S*:*MIR173* and *35S*:*173-GFP* or *35S*:*MIR171* and *35S*:*171-GFP* were analyzed for phasing as described (24). Radar plots to display phasing were generated as in Axtell *et al.* (25). tasiRNA and miRNA reads from Col-0 and *ago1–25* inflorescence tissue (flowers stages 1–12) were normalized to total unparsed reads in each library.

Statistical Analysis. Small RNA reads in individual libraries were normalized by using the total reads/library. S-PLUS (Insightful) and Excel (Microsoft) were used for all statistical tests and calculations. Bonferroni adjustments were made to significance level cutoffs when doing multiple comparisons.

1. Moissiard G, Parizotto EA, Himber C, Voinnet O (2007) Transitivity in *Arabidopsis* can be primed, requires the redundant action of the antiviral Dicer-like 4 and Dicer-like 2, and is compromised by viral-encoded suppressor proteins. *RNA* 13:1268–1278.

2. Ho SN, *et al.* (1989) Site-directed mutagenesis by overlap extension using the polymerase chain reaction. *Gene* 77:51–59.

3. Johansen LK, Carrington JC (2001) Silencing on the spot: Induction and suppression of RNA silencing in the *Agrobacterium*-mediated transient expression system. *Plant Physiol* 126:930–938.
4. Curtis MD, Grossniklaus U (2003) A gateway cloning vector set for high-throughput functional analysis of genes in planta. *Plant Physiol* 133:462–469.
5. Morel JB, *et al.* (2002) Fertile hypomorphic ARGONAUTE (ago1) mutants impaired in posttranscriptional gene silencing and virus resistance. *Plant Cell* 14:629–639.
6. Grigg SP, Canales C, Hay A, Tsiantis M (2005) SERRATE coordinates shoot meristem function and leaf axial patterning in *Arabidopsis*. *Nature* 437:1022–1026.
7. Allen E, Xie Z, Gustafson AM, Carrington JC (2005) microRNA-directed phasing during *trans*-acting siRNA biogenesis in plants. *Cell* 121:207–221.
8. Chen X, Liu J, Cheng Y, Jia D (2002) HEN1 functions pleiotropically in *Arabidopsis* development and acts in C function in the flower. *Development* 129:1085–1094.
9. Vazquez F, Gasciolli V, Crete P, Vaucheret H (2004) The nuclear dsRNA binding protein HYL1 is required for microRNA accumulation and plant development, but not post-transcriptional transgene silencing. *Curr Biol* 14:346–351.
10. Golden TA, *et al.* (2002) Short integuments1/suspensor1/carpel factory, a Dicer homolog, is a maternal effect gene required for embryo development in *Arabidopsis*. *Plant Physiol* 130:808–822.
11. Hunter C, Sun H, Poethig RS (2003) The *Arabidopsis* heterochronic gene *ZIPPY* is an ARGONAUTE family member. *Curr Biol* 13:1734–1739.
12. Xie Z, Allen E, Wilken A, Carrington JC (2005) DICER-LIKE 4 functions in trans-acting small interfering RNA biogenesis and vegetative phase change in *Arabidopsis thaliana*. *Proc Natl Acad Sci USA* 102:12984–12989.
13. Allen E, *et al.* (2004) Evolution of microRNA genes by inverted duplication of target gene sequences in *Arabidopsis thaliana*. *Nat Genet* 36:1282–1290.
14. Baumberger N, Baulcombe DC (2005) *Arabidopsis* ARGONAUTE1 is an RNA slicer that selectively recruits microRNAs and short interfering RNAs. *Proc Natl Acad Sci USA* 102:11928–11933.
15. Zilberman D, Cao X, Jacobsen SE (2003) ARGONAUTE4 control of locus-specific siRNA accumulation and DNA and histone methylation. *Science* 299:716–719.
16. Takeda A, *et al.* (2008) The mechanism selecting the guide strand from small RNA duplexes is different among argonaute proteins. *Plant Cell Physiol* 49:493–500.
17. Lobbes D, *et al.* (2006) SERRATE: A new player on the plant microRNA scene. *EMBO Rep* 7:1052–1058.
18. Zheng X, Zhu J, Kapoor A, Zhu JK (2007) Role of *Arabidopsis* AGO6 in siRNA accumulation, DNA methylation, and transcriptional gene silencing. *EMBO J* 26:1691–1701.
19. Alonso JM, *et al.* (2003) Genomewide insertional mutagenesis of *Arabidopsis thaliana*. *Science* 301:653–657.
20. Clough SJ, Bent AF (1998) Floral dip: A simplified method for *Agrobacterium*-mediated transformation of *Arabidopsis thaliana*. *Plant J* 16:735–743.
21. Llave C, Xie Z, Kasschau KD, Carrington JC (2002) Cleavage of Scarecrow-like mRNA targets directed by a class of *Arabidopsis* miRNA. *Science* 297:2053–2056.
22. Montgomery TA, *et al.* (2008) Specificity of ARGONAUTE7-miR390 interaction and dual functionality in TAS3 *trans*-acting siRNA formation. *Cell* 133:128–141.
23. Xie Z, *et al.* (2005) Expression of *Arabidopsis* MIRNA genes. *Plant Physiol* 138:2145–2154.
24. Howell MD, *et al.* (2007) Genomewide analysis of the RNA-DEPENDENT RNA POLYMERASE6/DICER-LIKE4 pathway in *Arabidopsis* reveals dependency on miRNA- and tasiRNA-directed targeting. *Plant Cell* 19:926–942.
25. Axtell MJ, Jan C, Rajagopalan R, Bartel DP (2006) A two-hit trigger for siRNA biogenesis in plants. *Cell* 127:565–577.

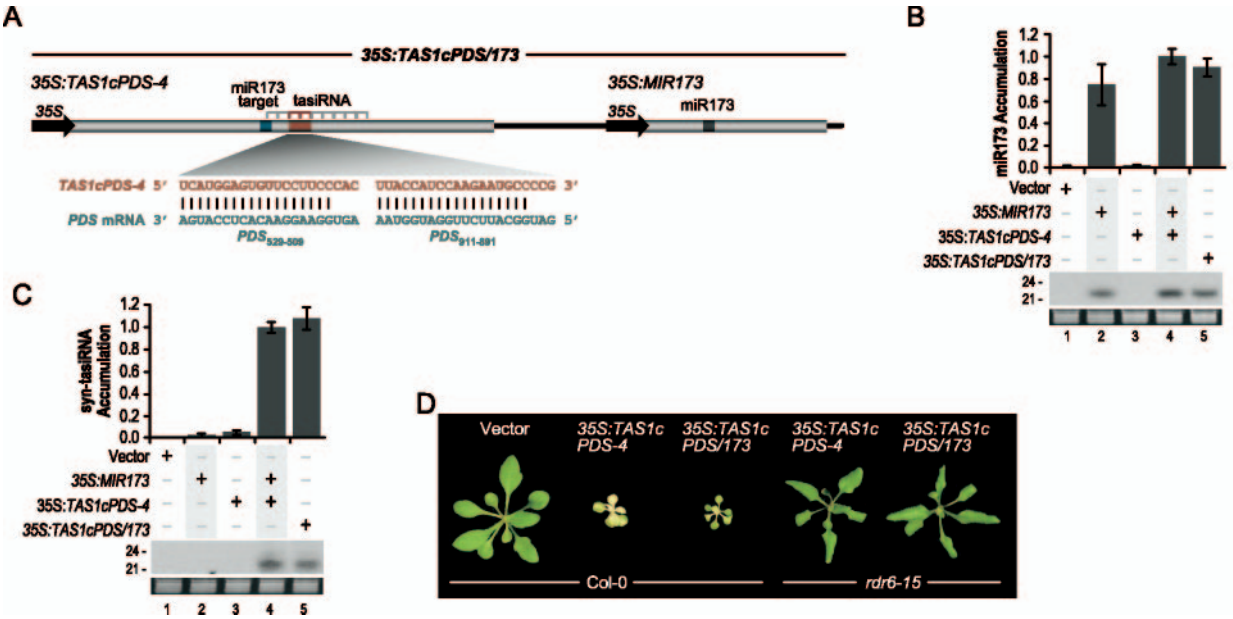

Fig. S1. syn-tasiRNA formation in *N. benthamiana*. (*A*) Organization of *35S:TAS1cPDS/MIR173*. (*B* and *C*) Mean relative level +/− SEM of miR173 and syn-tasiRNA in a transient assay in *N. benthamiana*, as determined by blot assays (*35S:TAS1cPDS-4* + *35S:MIR173* = 1.0). Small RNA blots for one of three biological replicates are shown. EtBr-stained 5S rRNA/tRNA are shown as a loading control. (*D*) Representative images of Col-0 and *rdr6–15* plants expressing syn-tasiRNA constructs.

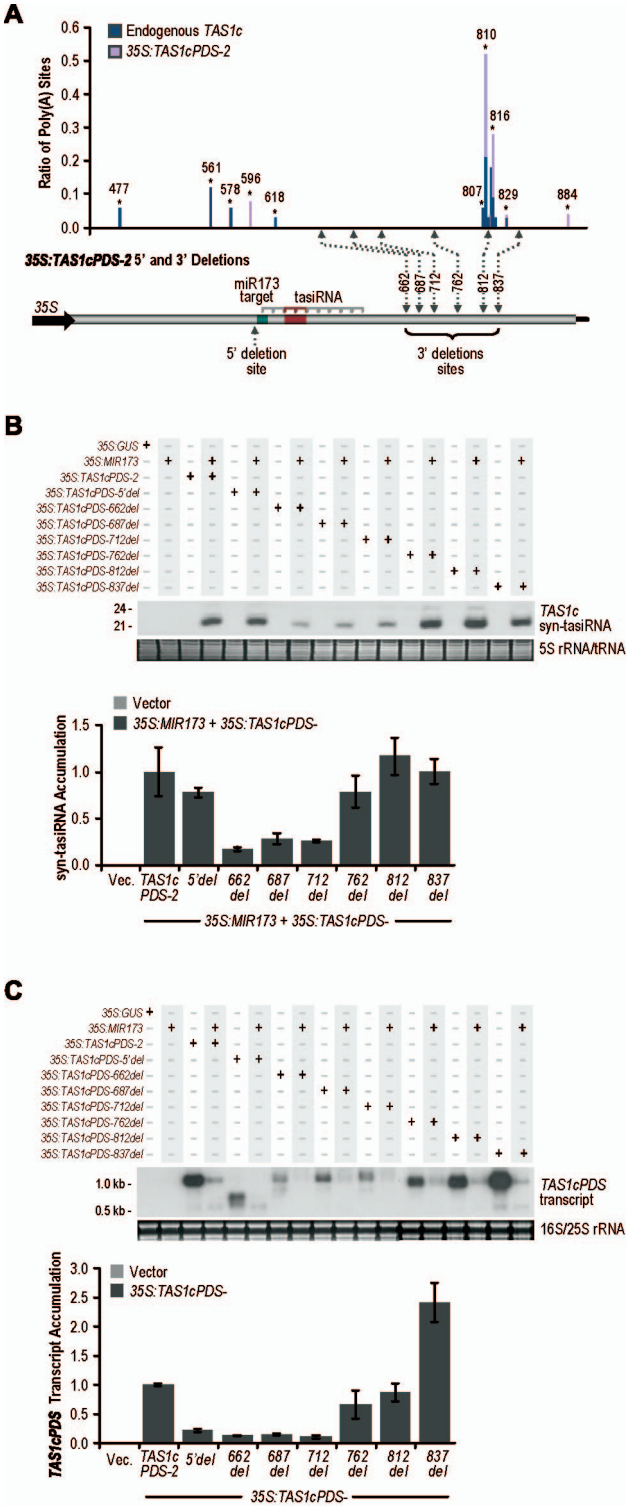

Fig. S2. The effect of 5′ and 3′ end deletions on syn-tasiRNA formation. (*A*) Mapping of authentic *TAS1c* and *35S:TAS1cPDS-2* primary transcript 3′ ends. The positions of 3′ ends were determined by 3′ RACE and nucleotide sequence analysis, with a minimum of 25 clones analyzed. The ratio of poly(A)-proximal sites at each position is indicated on the *y* axis. Arrows indicate the positions of 5′ and 3′ deletions. (*B* and *C*) syn-tasiRNA formation and primary transcript accumulation from *TAS1c*-based syn-tasiRNA constructs in the *N. benthamiana* transient expression assay. Constructs were expressed in the presence or absence of *35S:MIR173* as indicated above the blot panels. (*B*) Mean relative level +/− SEM of syn-tasiRNA as determined by blot assays (*35S:TAS1cPDS-2* + *35S:MIR173* = 1.0). One of three biological replicates is shown. EtBr-stained 5S rRNA/tRNA is shown as a loading control. (*C*) Mean relative level +/− SEM of primary *TAS1c*-based syn-tasiRNA transcripts (*35S:TAS1cPDS-2* = 1.0) for the same samples as shown in *B*. One of three biological replicates is shown. EtBr-stained 18S/25S rRNA is shown as a loading control.

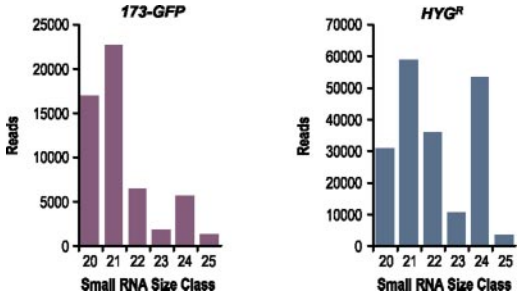

Fig. S3. Size distribution for small RNA reads matching perfectly to either *173-GFP* or *HYG*^{R} transcripts. The number of small RNA reads is shown for each of the 20- to 25-nt size classes.

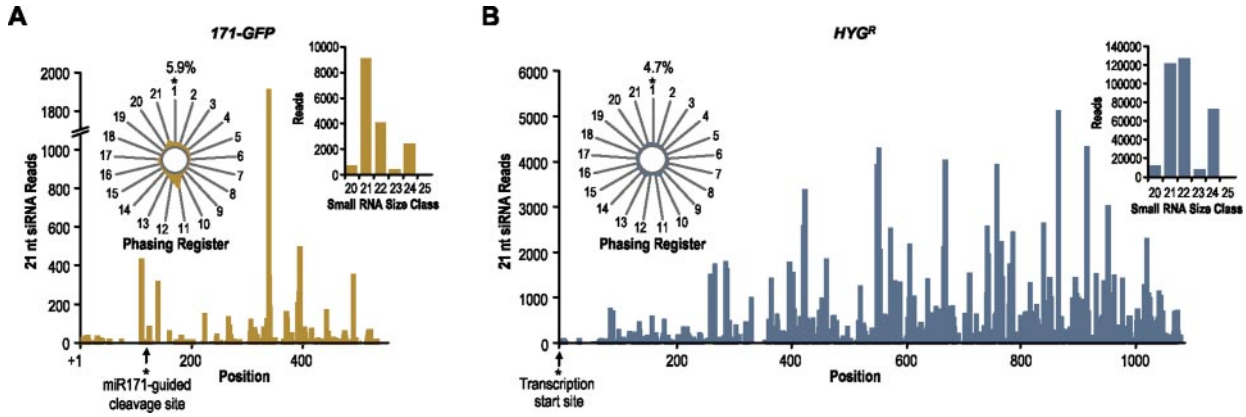

Fig. S4. Small RNA read distribution across *171-GFP* and *HYG*^{R} transcripts. Twenty-one-nucleotide small RNA reads matching perfectly to *171-GFP* (*A*) or *HYG*^{R} (*B*) transcripts. (*Inset*) Radar plots display percentages of reads corresponding to each of the 21 registers, with the 5′ end formed by miR171-guided cleavage or the transcription start site in *171-GFP* and *HYG*^{R}, respectively, defined as register 1. Bar plots display the number of small RNA reads for each of the 20- to 25-nt size classes.

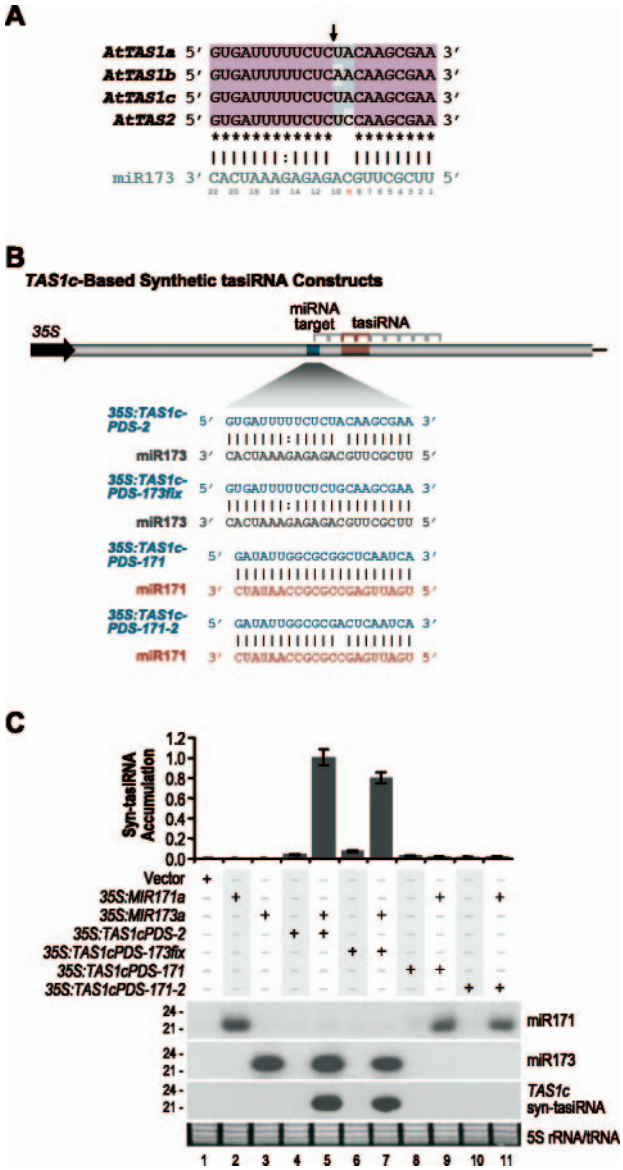

Fig. S5. Effect of mispairing at the miR173 target site in *35S:TAS1cPDS-2* on syn-tasiRNA formation. (*A*) Alignment of the miR173 target sites from *TAS1* and *TAS2* transcripts. The miR173-guided cleavage site is indicated by the arrow. (*B*) Organization of *35S:TAS1cPDS-2* and mutant constructs. (*C*) Mean relative level +/− SEM of syn-tasiRNA as determined by blot assays (*35S:TAS1cPDS-2* + *35S:MIR173* = 1.0). *TAS1c*-based syn-tasiRNA constructs containing authentic or mutated miR173 or miR171 target sites were expressed or coexpressed in *N. benthamiana* leaves as indicated above the blot panels. One of three biological replicates is shown. EtBr-stained 5S rRNA/tRNA is shown as a loading control.

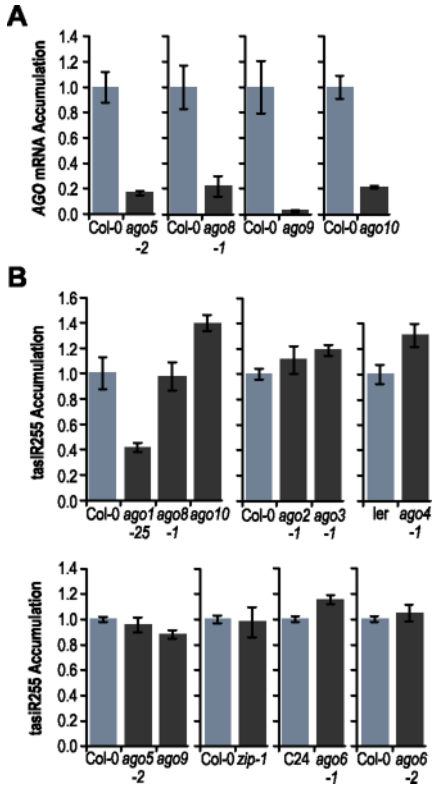

Fig. S6. *TAS1* tasiR255 levels in *AGO* mutants. (*A*) Blot assays for *AGO* mRNA. Mean relative level +/− SEM for each *AGO* mRNA as indicated (Col-0 = 1.0). (*B*) Blot assays for tasiR255. Mean relative level +/− SEM of tasiR255 (Col-0, ler, or C24 = 1.0).

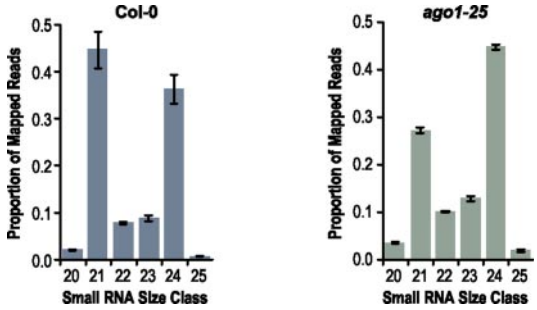

Fig. S7. Size distribution for small RNA reads from Col-0 and *ago1–25*. The mean proportion +/− SEM of total 20- to 25-nt small RNA reads is shown for each size class.

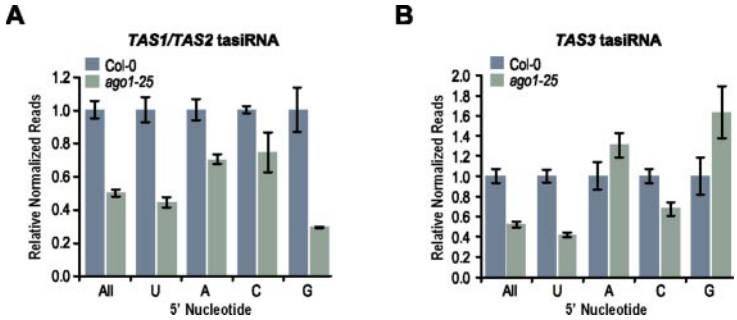

Fig. S8. Deep sequencing analysis of AGO1-dependent tasiRNA. (*A*) Mean relative level +/− SEM of *TAS1* and *TAS2* tasiRNA based on the 5′ nt (Col-0 = 1.0). (*B*) Mean relative level +/− SEM of *TAS3* tasiRNA based on the 5′ nt (Col-0 = 1.0).

Other Supporting Information Files

Table S1
Table S2
Table S3
Table S4
Table S5
Table S6
Table S7
Table S8